Available online at www.sciencedirect.com
SCIENCE DIRECT®
ELSEVIER
Applied Acoustics 64 (2003) 917–930
applied acoustics
www.elsevier.com/locate/apacoust

A preliminary study of an isodynamic transducer for use in active acoustic materials

Hervé Lissek[a,*], Xavier Meynial[b]

[a]*Centre Scientifique et Technique du Bâtiment, F- 38400 Saint-Martin d'Hères, France*
[b]*Laboratoire d'Acoustique de l'Université du Maine, F-72085 Le Mans, France*

Received 18 June 2002; received in revised form 27 January 2003; accepted 28 January 2003

Abstract

Active control of the acoustic impedance of walls in rooms allows fine control of the reverberation in auditoria. Such active materials may use locally reacting cells comprising a transducer connected to an electronic control circuit. In this paper, a simple feedback circuit based on a linear combination of the pressure at the transducer diaphragm and the velocity of the diaphragm is presented. We then discuss the desired characteristics of a transducer dedicated to our application, and show that the isodynamic technology is an interesting candidate, especially if using rubber magnet bars. We present results from simulations involving a finite element model of such transducer, which predict a good control over two frequency decades. Preliminary experimental results obtained with a basic prototype of isodynamic transducer are encouraging, yielding an absorption coefficient approaching 1 (>0.7) from 30 up to 500 Hz. We think that far better results can be obtained (specially in the "super-reflecting" case) with closer control over the various mechanical parameters. Future work will also address the optimisation of the magnet geometry.

Keywords: Room acoustics; Electroacoustics; Active impedance control; Isodynamic transducers

1. Introduction

Active reverberation enhancement systems have been on the market since the late sixties. These systems were first aiming at increasing reverberation time, but they are now capable of altering (to a certian extent) other aspects of reverberation, such as early to late energy ratios. However, their possibilities are limited by the fact that

* Corresponding author.
E-mail addresses: herve.lissek@libertysurf.fr (H. Lissek), active.audio@wanadoo.fr (X. Meynial).

0003-682X/03/$ - see front matter © 2003 Elsevier Science Ltd. All rights reserved.
doi:10.1016/S0003-682X(03)00022-7

they are only able to add energy in the room, but not to absorb energy. As a consequence, they are sometimes criticised for excessive sound levels. A number of systems are now on the market [1,2], which use traditional sound reinforcement devices such as microphones, digital signal processing, amplifiers and loudspeakers. The commercial success of these systems is questionnable: less than 200 systems have been installed over the world.

In 1985, Guicking introduced the intuitive idea of the active wall [3] illustrated by Fig. 1. An active wall is an array of locally reacting cells, each cell comprising a sensor, an electronic control circuit, and an actuator. A single reciprocal transducer may in fact act both as a sensor and an actuator. In a previous paper [4], we have reported results obtained with a standard (hifi type) electrodynamic dome tweeter connected to an impedance bridge. Reflection coefficients ranging from nearly 0 to more than 2 (in the following, a reflection coefficient greater than one will be referred to as "super-reflection") were obtained in a tube around the resonance frequency of the transducer. However, the bandwidth of the control was much too narrow for our application. In a later paper [5], we presented a work on a double feedback scheme similar to Darlington's [6] which could broaden the bandwidth. The feedback is a linear combination of the velocity of the transducer diaphragm and the acoustic pressure at the diaphragm / air interface.

Then we looked at the problem of interaction between cells of an active wall [7] and showed that for reasonable values of reflection coefficients, this phenomenon is not likely to cause instability of the cells.

The present paper focuses on the study of a transducer dedicated to our application. We first analyse the behaviour of the system and show that the isodynamic transducer is a good both from its electroacoustical properties and manufacturing standpoint. We then present preliminary experimental results obtained with these transducers.

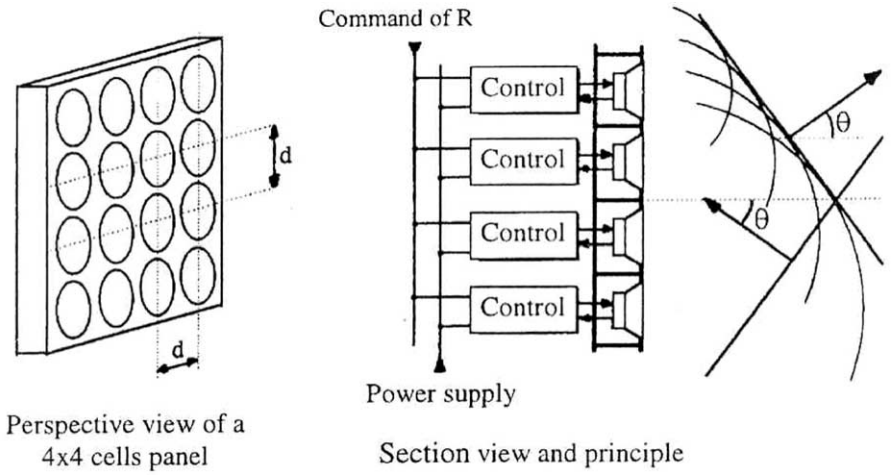

Fig. 1. Principle of the active wall, consisting in an array of locally reacting cells.

2. Specifications of the active transducer

The tranducer is represented by a two-port network (A, B, C, D) where P is the pressure at the diaphragm, Q the volume flow generated on one side of the diaphragm, U and I, the voltage and current, respectively, in the coil (on the other side). In the following, we restrict ourselves to the case of electrodynamic transducers. Considering the Thiele–Small model, we have

$$\begin{bmatrix} U \\ I \end{bmatrix} = \begin{bmatrix} A & B \\ C & D \end{bmatrix} \cdot \begin{bmatrix} P \\ Q \end{bmatrix} \quad \text{with} \quad \begin{bmatrix} A & B \\ C & D \end{bmatrix} = \begin{bmatrix} -Z_e \cdot \dfrac{S}{Bl} & -\dfrac{Bl}{S} - \dfrac{Z_e . Z_m}{S.Bl} \\ -\dfrac{S}{Bl} & -\dfrac{Z_m}{S.Bl} \end{bmatrix},$$

where Z_e is the electrical impedance of the transducer consisting of a resistor R_e in series with an inductance L_e, Z_m is the mechanical impedance of the transducer consisting of a mass M_m in series with a compliance C_m and a resistor R_m, S is the surface of the diaphragm, and Bl, the force factor.

The transducer is connected to an impedance bridge consisting of three other impedances Z_0, Z'_0, and Z'_1 as shown in Fig. 2. The pressure P at the transducer diaphragm is measured by a microphone, its output voltage added to the differential voltage V_d of the bridge, and fed back to the bridge after filtering and amplification according to:

$$V_{CR} = \Gamma_1 . P + \Gamma_2 . V_d \tag{1}$$

where Γ_1 and Γ_2 represent the gains of amplification associated with the pressure P and the voltage V_d, respectively.

The simplicity of the control circuit must be emphasised. It should also be mentioned that the pressure capture could also be performed using a second impedance bridge [8], thus avoiding the need for a microphone.

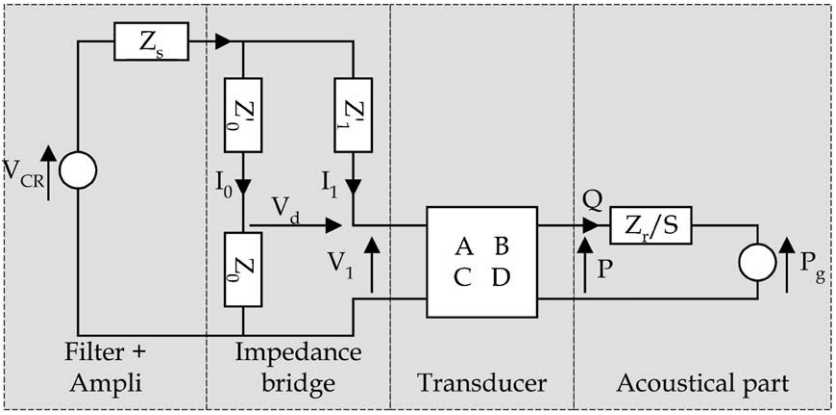

Fig. 2. Electrical circuit equivalent to one cell of the active wall. Feedback: $V_{CR} = \Gamma_1 . P + \Gamma_2 . V_d$.

The output impedance of the power amplifier is denoted Z_s. In the following, we shall neglect Z_s for the sake of simplicity (in most cases, the values of the resistors in the bridge are much greater than the value of impedance Z_s).

If $Z_0 = Z'_0$ and $Z'_1 = Z_e$, V_d is directly proportionnal to the velocity V of the membrane (assuming it behaves as a piston), and the feedback signal is a linear combination of P and V as explained in [6]. In this case, the volume flow Q of the diaphragm equals $S.V$, and Z_r/S is the radiation impedance of the transducer.

2.1. Acoustic impedance of a cell

The acoustic impedance $Z_a = -S.P/Q$ presented by the transducer to an inpinging wave is related to the plane wave reflection coefficient at normal incidence R, according to $R = (Z_a - Z_c)/(Z_a + Z_c)$, where Z_c is the characteristic impedance of plane waves, $Z_c \approx \rho.c = 408$ N.s/m^3.

It can be shown that, if $Z_0 = Z'_0$, $Z'_1 = Z_e$, $Z_s = 0$, and $\Gamma_2 > > 2$, then [9]

$$Z_a(\omega) = Z_{ad}.\frac{4Z_m - (\Gamma_2 - 2)(Bl)^2/Z_e}{4S.Z_{ad} - (\Gamma_2 - 2)(Bl)^2/Z_e} \approx Z_{ad}.\frac{4Z_m - \Gamma_2(Bl)^2/Z_e}{4S.Z_{ad} - \Gamma_2(Bl)^2/Z_e} \tag{2}$$

where $Z_{ad} = Bl.\frac{2-\Gamma_2}{2.\Gamma_1} \approx -Bl.\frac{\Gamma_2}{2.\Gamma_1}$ is the desired acoustic impedance expression in terms of ratio Γ_2/Γ_1. The desired reflection coefficient expression in terms of Z_{ad} (or ratio Γ_2/Γ_1) becomes $R_d = \frac{Z_{ad}-Z_c}{Z_{ad}+Z_c}$.

If $|\Gamma_2.(Bl)^2/Z_e| \gg |4Z_m|$ and $|\Gamma_2.(Bl)^2/Z_e| \gg |4S.Z_{ad}|$, then $Z_a \approx Z_{ad}$. The frequency bandwidth of the impedance control is dependent on these two conditions. Around the transducer resonance frequency f_S, $|Z_m|$ is minimum. In this case, as $|S.Z_{ad}|$ is usually rather smaller, (for $|R_d| = 0$, we have $Z_{ad} = Z_c$, and for $|R_d| = 2$, we have $Z_{ad} = -3Z_c$ or $-Z_c/3$), the performance of the control is optimum. As can be seen, the choice of the transducer is mainly based on the maximisation of the ratio $|(Bl)^2/(Z_e Z_m)|$.

Obviously, a wide bandwidth will be obtained with transducers having a large ratio $(Bl)^2/R_e$. The inductance L_e will tend to reduce the bandwidth as it increases $|Z_e|$ at high frequencies. Finally, the ideal transducer should have a small mechanical impedance, i.e. low moving mass M_m and high compliance C_m (the value of R_m is not critical in practice).

Figs. 3 and 4 show the reflection coefficient R and the open-loop gain T (see below) predicted for a 37 mm dome tweeter (Audax TW37Y0) with a resonance frequency $f_S = 719$ Hz. The modulus of the reflection coefficient $|R|$ is plotted versus frequency and Γ_2. The open-loop gain T is plotted versus frequency at $\Gamma_2 = 100$. Figs. 3 and 4 correspond to a desired reflection coefficient $|R_d| = 0$ and $|R_d| = 2$, respectively. It can be seen that the bandwidth increases with Γ_2.

Another feature, specific to our application, concerns power requirements: assuming a plane wave of maximum sound pressure level, SPL = 100 dB, the impinging power flux per square meter is 10 mW/m^2. Then, the energy radiated by a 10×10 cm^2 cell with $|R| = 2$ is 0.2 mW; assuming a 1% efficiency, the electrical

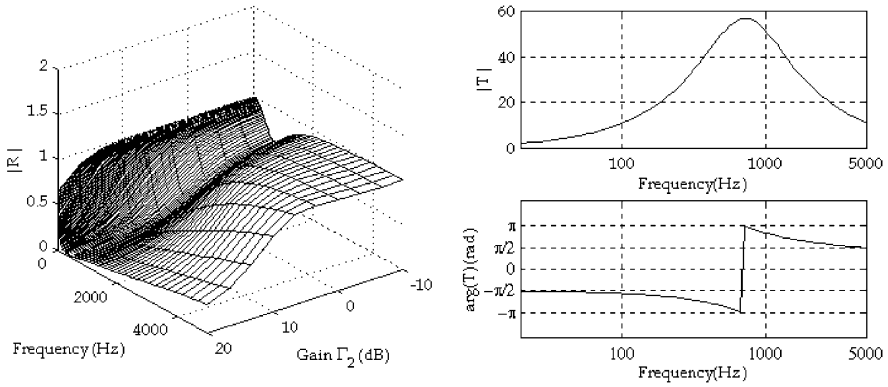

Fig. 3. Prediction of the modulus of the reflection coefficient versus frequency and Γ_2 (left), and the open-loop gain versus frequency for $\Gamma_2 = 100$ (right) for a desired reflection coefficient $|R_d| = 0$, using a dome tweeter having a resonance $f_S = 719$ Hz.

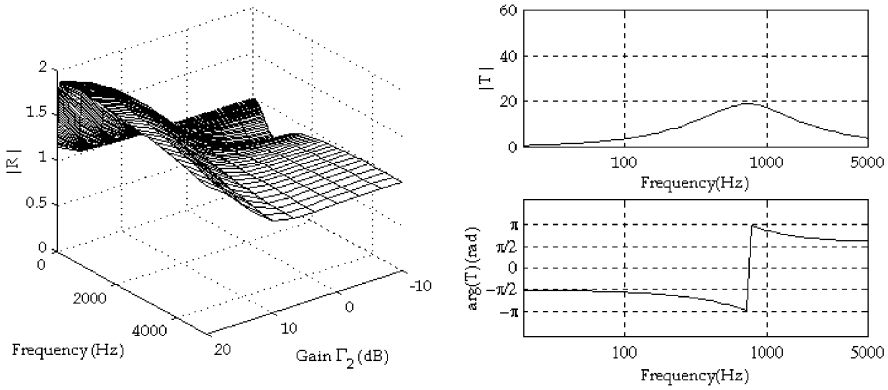

Fig. 4. As for Fig. 3, but with $|R_d| = 2$.

power of the cell is 20 mW. This very low power specification allows the use of very thin (and low mass) conductors.

2.2. Stability of a cell

Assuming the same conditions as above, i.e. $Z'_1 = Z_e$, $Z_s = 0$, and $\Gamma_2 >> 2$, the open-loop gain of the system can be expressed as [8,9]:

$$T = Bl.\frac{Bl.\dfrac{\Gamma_2}{2} - \Gamma_1.Z_r}{2.Z_e.(Z_m + S.Z_r) + Bl^2} = Bl.\Gamma_1.\frac{-Z_{ad} - .Z_r}{2.Z_e.(Z_m + S.Z_r) + Bl^2}$$
$$\approx \frac{\Gamma_2}{2}.\frac{1 + Z_r/Z_{ad}}{1 + 2.\dfrac{Z_e}{Bl^2}.Z_m} \tag{3}$$

Considering several adjacent cells, the radiation impedance Z_r of each transducer depends on coupling between cells. In practice, coupling can be neglected as shown in [7], and Z_r can be approximated as the radiation impedance of a piston in a half space. In this case, we have, at low frequencies, $|Z_r/Z_{ad}| \ll 1$ for typical values of $|R|$ (see previous paragraph).

At the transducer resonance frequency, the second ratio in (3) is real and positive for any given Γ_2/Γ_1 ratio (i.e. any given acoustic impedance), and the negative values of Γ_2 ensure maximum stability [$Arg(T) \approx \pi$] as can be seen on Figs. 3 and 4. The transducer mechanical impedance $|Z_m|$ increases as frequency departs from f_S, so that T approaches $\Gamma_2.(Bl)^2/(Z_e.Z_m)$: $|T|$ decreases and $Arg(T)$ tends towards $-\pi/2$ at low frequencies, and $+\pi/2$ at high frequencies if we neglect the influence of L_e (0 if we take L_e into account). It is clear that we want L_e to be as small as possible, so that $|T|$ is minimum when $Arg(T)$ approaches 0. A low moving mass keeps $|T|$ high, but also ensures maximum phase margin, so that it is not a penalty.

In practice, $Arg(T)$ approaches 0 at high frequencies due to the non-zero distance between the transducer and the microphone, the frequency dependence of Z_r, the various cut-off in the electronic circuitry, secondary resonances and various phenomena in the transducer. All these phenomena make it difficult to predict accurately the stability at high frequencies. No stability problems are expected at low frequencies.

The critical factor in Eqs. (2) and (3) is $\Gamma_2.(Bl)^2$, rather than $(Bl)^2$. Therefore, small values for Bl can be compensated by large values of Γ_2. However, very large values of Γ_2 could also yield excessive background noise and cost for the electronic circuit.

Very low moving mass can be obtained with electrostatic transducers, but we rejected them due to a number of disadvantages (very high voltage excitation due to poor efficiency, capacitive electrical impedance, sensibility to dust,...). The same applies to PVDF transducers.

3. Isodynamic transducers

The conclusions drawn in the previous section suggest that isodynamic transducers can provide an effective alternative to the conventional cone speaker. These devices use electrodynamic transduction and offer the advantage of low moving mass (because the membrane is a flexible film and not a rigid cone). This type of transducer is shown in Figs. 5 and 6 along with a representation of the magnetic flux lines.

Another advantage of the isodynamic transducer is that its topology is well suited for low cost manufacturing of large panels using rubber magnets. With such magnets, inductions in the order of 0.3 T can be achieved along the electrical conductors. The membrane can be made of kapton film (25 μm thick in our prototypes), with deposited aluminium or copper tracks (20 μm thick in our prototypes).

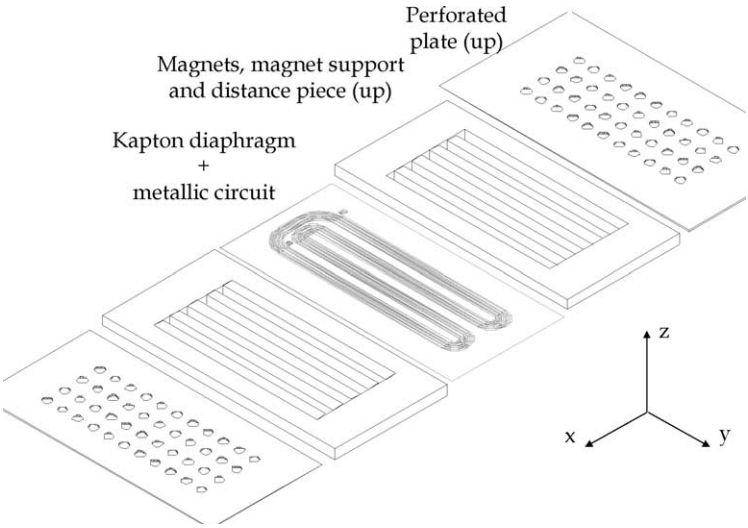

Fig. 5. Isodynamic transducer.

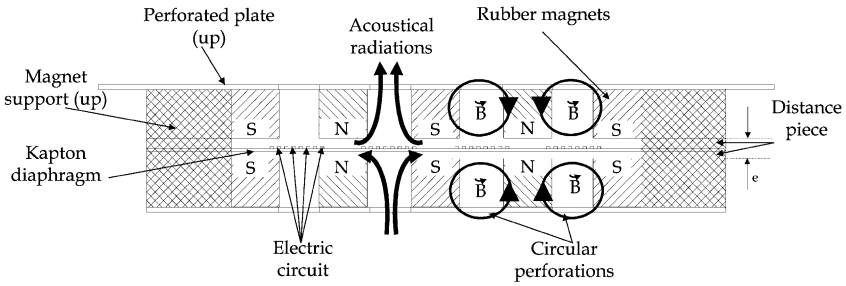

Fig. 6. Section view of the isodynamic transducer.

3.1. Modelling

A finite element model of this type of transducer was used to predict the displacement of its membrane. It is a two-dimensional model based on the assumption that the transducer has infinite length along the y direction (see Fig. 5). The model uses parabolic elements. The main difficulty in modelling this transducer is to take into account the mass M_V and resistance R_V associated with the movement of the air in the thin slots between the membrane and the magnets. This mass turns out to be of primary importance in practice. In addition, thin stabilising stripes of elastic/absorbtive elements can be placed between the membrane and the magnets in order to shift the resonances towards high frequencies and damp them.

The overall volume flow Q is integrated, leading to the membrane velocity. The equivalent two-port network (A, B, C, D) is estimated from the above finite element model (and fed into the model of Fig. 2). Details about the model can be found in [9].

Obviously, a small value e (magnet gap width, see Fig. 6) is required for a large value of induction B. But this is conflicting with the behaviour of the mass M_V, which increases as e decreases, so that a compromise must be found. The balance between e and B is one of the critical aspects in the design of a suitable transducer for our application. Future work will have to investigate this issue in detail, by using for instance magnets with non-rectangular section. For example, with our 200 cm^2 prototype transducer (see below), the first resonance frequency is shifted from 140 Hz when the transducer is not loaded with air (vacuum) down to 70 Hz when it is loaded with air, leading to an equivalent mass of 8.1g which severely impairs the advantages of the isodynamic transducer.

3.2. Simulation results

Figs. 7–9 show the simulation of the absorption coefficient $(\alpha = 1 - |R|^2)$ obtained for plane waves under normal incidence, for the two desired reflection coefficients, $|R_d| = 0$ and $|R_d| = 2$. These results are compared to the ones obtained for a passive transducer, i.e. the control is off. The transducer has the following characteristics:

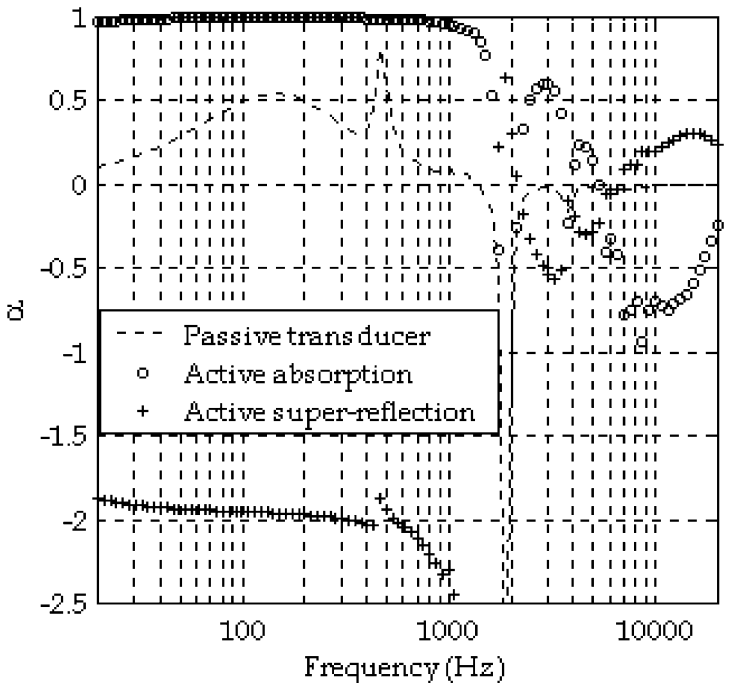

Fig. 7. Predicted absorption coefficient with influence of M_V neglected. Active absorption: $\Gamma_1 = 1$V/Pa, $\Gamma_2 = -550$; active super-reflection: $\Gamma_1 = -1$V/Pa, $\Gamma_2 = -1500$.

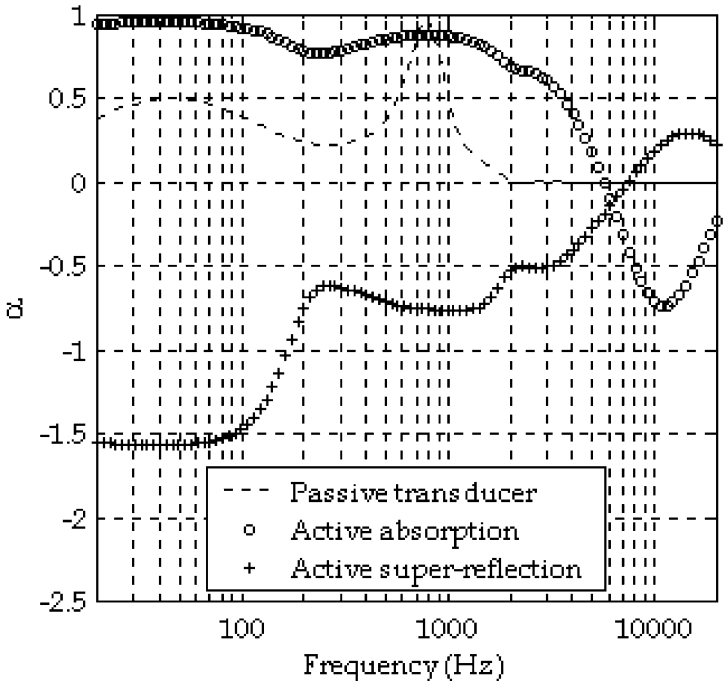

Fig. 8. (Below left): Predicted absorption coefficient with influence of M_V taken into account. No stabilising stripes. Same gains.

a membrane made of kapton, 25 μm thick, surface of 175×85 mm.
Two rows of 5 bars of rubber magnet, with section 10×10 mm, and a gap width $e = 1$ mm; 12 mm between adjacent bars; volume between magnet bars $V_{\text{air gap}} = 20$ cm^3.
For the electrical circuit: four bands made of copper (as in Fig. 5) each band comprising 16 tracks, with section 600×36 μm, leading to a total moving mass $M_m = 2.7$ g and a $Bl = 4.3$ T.m.
For the acoustic radiation: four rows of 11 holes 8.5 mm on each supporting plate.

In Fig. 7, the influence of M_V has been neglected. It can be seen that the control performs from 20 to 1500 Hz. Around 500 Hz and around 2 kHz, the model fails to predict the behaviour of the passive transducer. This limitation is due to singularities occurring at frequencies related to the dimensions of the transducer. However, the overall behaviour is predicted correctly, as the comparison with experimental results will show.

In Fig. 8, the mass M_v is now taken into account. In this case, the bandwidth of the control is limited at high frequencies, especially for $|R_d| = 2$. Finally, the introduction of two stabilising stripes (Fig. 9) increases the bandwidth at high frequencies (the resonances are shifted towards high frequencies). However, M_v limits the

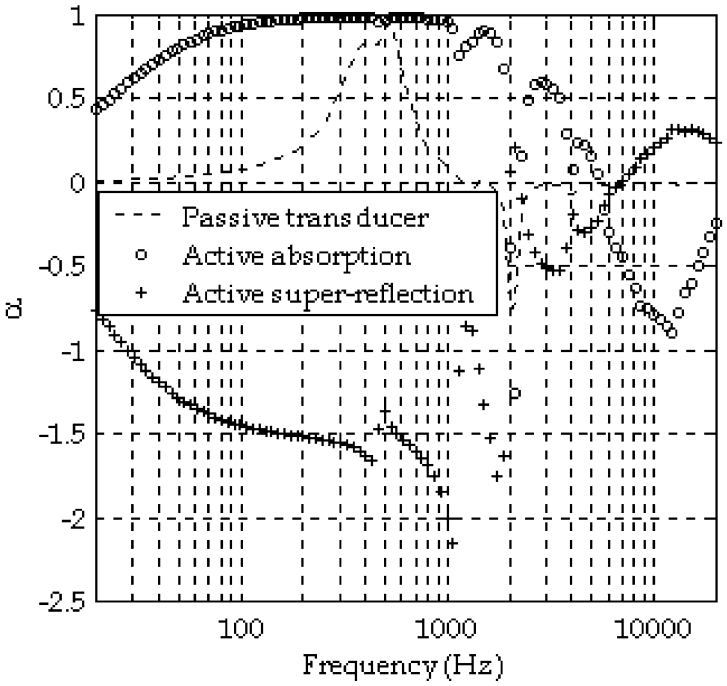

Fig. 9. Predicted absorption coefficient with influence of M_V taken into account. Two stabilising stripes below 2nd and 4th magnet bars. Some gains.

bandwidth at low frequencies. In the latter case, the half-efficiency bandwidth ranges from around 25 Hz up to around 2 kHz in the case $|R_d| = 0$, and from 25 Hz to 1 kHz for the case $|R_d| = 2$.

Fig. 10 shows the open-loop gain T corresponding to the absorption case of Fig. 9. In this case, the phase margin is greater than 110°.

4. Experimental results

Several prototypes were made but the following discussion will be restricted to prototype "B16". This prototype has four bands of 16 copper tracks, each of section 600×36 μm, leading to a total moving mass $M_m = 2.7$ g, an estimated force factor $Bl = 4.3$ T.m, and a resistance $R_e = 13$ Ω. Each of the two supporting plates ("perforated plates" shown in Fig. 6) is perforated with 4×11 holes with 8.5 mm diameter. The spacing between adjacent magnet bars is 12 mm wide, and the bar height is 10 mm. Unfortunately, we were not able to control accurately important parameters such as the membrane strain and the mechanical behaviour of the stabilising stripes, so that in fact we had to abandon the use of such stripes. The results below should therefore be considered as preliminary, and we think that far better results

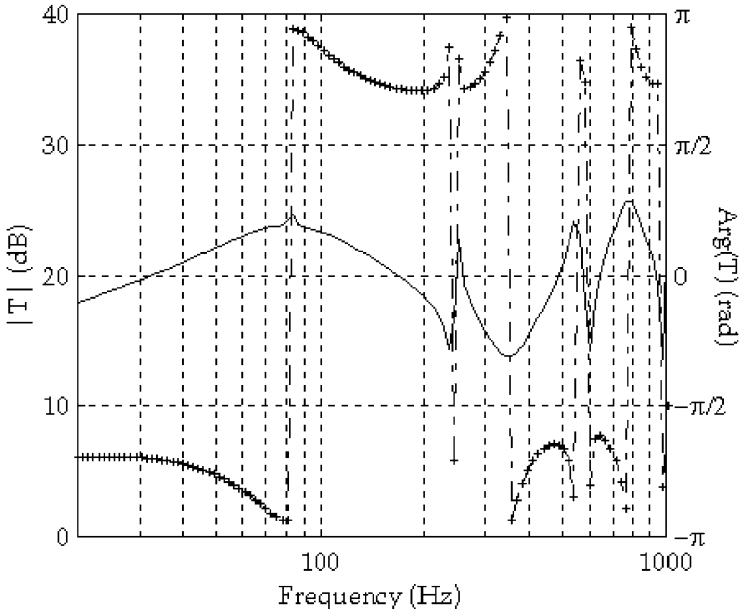

Fig. 10. Predicted open loop gain corresponding to the absorption case in Fig. 9. Same gains. Solid: modulus; + + + phase.

will be obtained with a better control of the manufacturing process. The purpose of the present preliminary study mainly consists in validating the choice of the isodynamic transducer.

Fig. 11 shows the electrical impedance of the transducer measured with and without air load. The influence of the mass M_V can be seen on the shift of the first resonance frequency. Impedance peaks are lower in the air-loaded case due to the added acoustic resistance R_V.

The impedance bridge is purely resistive $Z_0 = Z'_0 = R_0 = 10\ \Omega$, $Z'_1 = R_1 = 13\ \Omega$, and the pressure signal is obtained from a low-cost electret microphone (6.5 mm diameter), mounted on the rigid plate of the transducer. The microphone is located above one of the plate perforations, 10 mm above the vibrating membrane. The absorption coefficient of the prototype (with feedback control as described in Section 1) was measured using the Kundt tube method [10] using a sweep sine excitation.

Results are shown in Fig. 12, for three different cases: no feedback, feedback with $e = 4$ mm, and feedback with $e = 1.6$ mm (smaller gaps were difficult to reach due to lack of proper tools). As shown in the plot, the transducer without feedback (passive) is already rather absorptive, with α around 0.5. However, feedback control with $e = 4$ mm increases the absortion substantially: $\alpha > 0.7$ from 30 up to 500 Hz. Results obtained with $e = 1.6$ mm show decreased performances, especially at low frequencies. This could be explained by the increased mass M_v, However, raising M_V

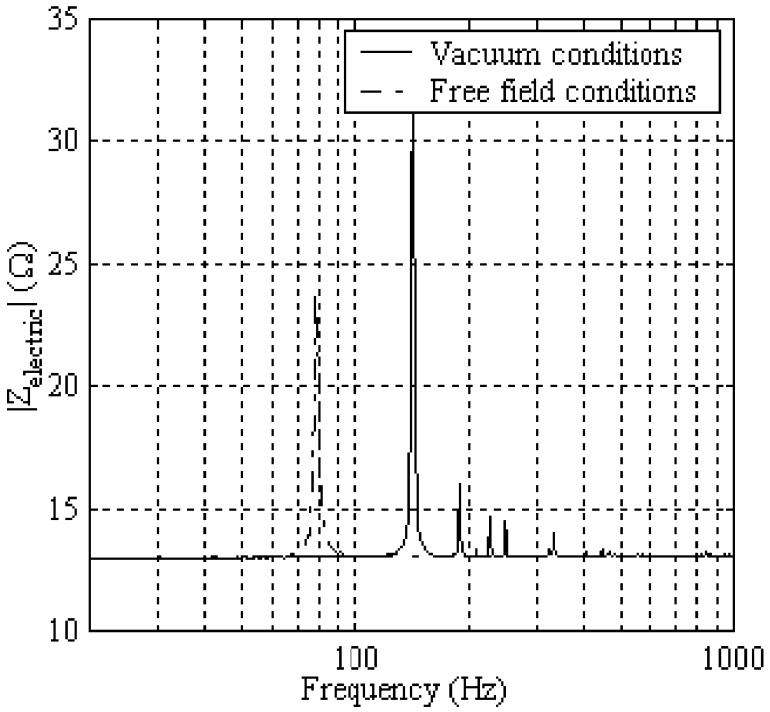

Fig. 11. Measured electrical impedance of isodynamic transducer prototype B16. Solid line: transducer not loaded with air (vacuum); dashed line: transducer loaded with air (in a screen in free space).

should affect high frequencies more than low frequencies. We think that the problem comes from a non-flat membrane due to poor control of the membrane strain when making the prototype. This problem is more likely due to the non-flat membrane: proper control of the membrane stress could not be achieved when making the prototype.

The open loop gain T corresponding to the result of Fig. 12 is shown in Fig. 13. Its phase, Arg(T) tends to $-\pi/2$ at low frequencies, and oscillates around $\pm\pi$ at high frequencies, resulting in an excellent stability.

5. Conclusions and future work

We have shown that the desired characteristics of a transducer dedicated to active materials with variable acoustic properties : low moving mass M_m, high $(Bl)^2/R_e$ factor, low electrical inductance L_e, low power capacity, and low-cost manufacturing for use in large pannels.

The above properties are best achieved with isodynamic transducers using rubber magnets. We have set up a finite element model of such transducer. The simulation results show that accurate impedance control can be obtained over two frequency

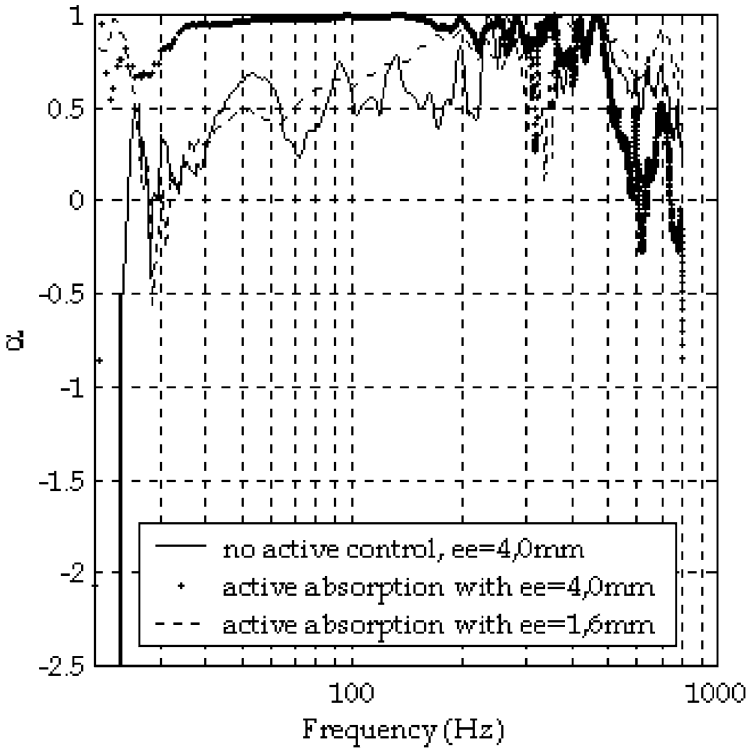

Fig. 12. Plane wave normal incidence absorption coefficient α obtained with prototype B16 and $|R_d| = 0$ using the Kundt tube method, with $\Gamma_1 = 1$V/Pa, $\Gamma_2 = -128$.

decades. Results also show that future work should focus on the problem of minimising the acoustic mass M_V which is related to the movement of the air in the thin slots between the membrane and the magnets. Solutions could involve grooves in the magnets, or non-rectangular section magnets for instance.

We have built and tested simple prototypes. Results are not as good as expected due to poor control over the membrane strain. Moreover, our limited manufacturing facility did not allow the testing of the stabilising stripes (between the magnet bars and the membrane) which would certainly have lead to better results. Good results could not be reached in the super-reflection case for the aforementioned reasons. We were unfortunately not able to obtain interesting results in the super-reflecting case ($|R_d| > 1$) due to our limited experimental means as stated above.

However, absorption coefficient greater than 0.7 could be achieved from 30 to 500 Hz (4 octaves). We see this result as rather encouraging, and we think it validates our choice of the isodynamic transducer.

Future work will address the minimisation of the additional acoustic mass M_V, and the exerimental control of the membrane strain and the stabilising stripes. The pressure sensing using a second impedance bridge instead of a microphone should also be addressed, along with the problem of background noise.

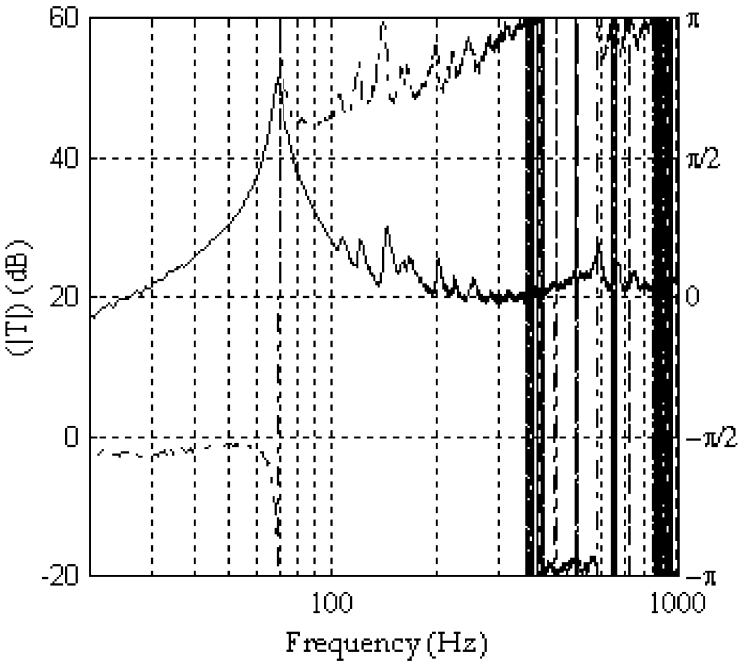

Fig. 13. Open-loop gain obtained with prototype B16, set for $|R_d| = 0$, with $\Gamma_1 = 1$V/Pa, $\Gamma_2 = -128$ [solid line: $|T|$ in dB; dashed line: $Arg(T)$ in rad].

References

[1] Kleiner M, Svensson P. Review of active systems in room acoustics and electroacoustics. Proc. ACTIVE 95, Newport Beach, CA., 1995. p. 39–54.
[2] Meynial X, Vian J-P. Active walls for room acoustics. Proc. of the International Convention on Sound Design, Karlsruhe, Germany, 1998. p. 134–41.
[3] Guicking D, Karcher K, Rollage M. Coherent active method for application in room acoustics. Journal of the Acoustical Society of America 1985;78(4):1426–34.
[4] Meynial X. Active materials for application in room acoustics. 3rd ICIM/ECSSM '96, Lyon, 1996. p. 968–73.
[5] Meynial, X, Lissek H. Active reflectors for room acoustics. Proc of the IOA 1999;21(6):99–107.
[6] Darlington P. Loudspeaker circuit with means for monitoring the pressure at the speaker diaphragm, means for monitoring the velocity of the speaker diaphragm and a feedback circuit. Int. patent no. PCT/WO97/03536, 1987.
[7] Lissek H, Meynial X. Le problème du couplage intercellulaire dans un mur actif. Proc. of the 5th C.F.A.. lausanne: Presses Polytechniques et Universitaires Romandes; 2000.
[8] Meynial X. Dispositif de contrôle actif d'impédance acoustique. Patent no. 9805953, 1998.
[9] Lissek H. Les matériaux actifs à propriétés acoustiques variables. PhD thesis, Université du Maine, 2002.
[10] Chu WT. Transfer function technique for impedance and absorption measurements in an impedance tube using a single microphone. Journal of the Acoustical Society of America 1986;80(2):555–60.